Initial Rotor Position Estimation for Brushless Synchronous Starter/Generators

Shuai Mao
School of Automation
Northwestern Polytechnical University
Xi'an, China
Email: maoshuai1989@gmail.com

Weiguo Liu
School of Automation
Northwestern Polytechnical University
Xi'an, China
Email: lwglll@nwpu.edu.cn

Jichang Peng
School of Automation
Northwestern Polytechnical University
Xi'an, China
Email: linkpjc@gmail.com

Ningfei Jiao
School of Automation
Northwestern Polytechnical University
Xi'an, China
Email: jiaoningfei@gmail.com

Yu Jiang
AVIC Shaanxi Aero Electric Co., Ltd.
Xi'an, China
Email: jiang115yu@163.com

***Abstract*—In this paper, an initial rotor position estimation method that is independent of the magnetic saliency is proposed for the main generator (MG) of the brushless synchronous starter/generator (BSSG). The stator of the MG works as a transmitter and the rotor of the MG works as a receiver, i.e., signals are injected into the stator windings and response signals of the field winding are regarded as indicators of the initial rotor position of the MG. Due to the brushless structure, direct measurement of the field winding of the MG is difficult. Thus, a practical approach to estimate the information of the field winding of the MG is proposed in this paper. Then, the initial rotor position of the MG is estimated with signal injection. The effectiveness of this method is verified by experimental results.**

I. Introduction

The brushless synchronous starter/generator (BSSG), which is highly reliable and inherently safe, is widely adopted by the integrated starter/generator system [1]–[7]. The structure of the three-stage BSSG is shown in Fig. 1. Three machines, a pre-exciter (PE), a main exciter (ME) and a main generator (MG), and a rotating rectifier are mounted on the same shaft.

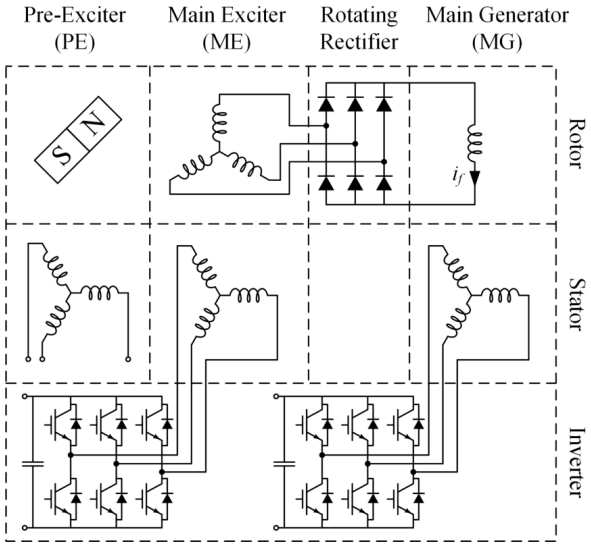

Fig. 1. Structure of the three-stage BSSG.

The initial rotor position of the MG is essential for sensorless start control of the BSSG [8]–[10]. Many initial rotor position estimation methods have been proposed, especially for permanent magnet synchronous motors (PMSMs). The magnetic saliency, an indicator of the rotor position, of the PMSM is usually detected by signal injection. The stator of the PMSM is both a transmitter and a receiver, i.e., signals are injected into the stator windings and response signals of the stator windings are analyzed to estimate the initial rotor position of the PMSM. In general, the magnetic saliency of the PMSM is stable, so the estimation results are reliable. Compared with the PMSM, the magnetic saliency of the MG is variable. Consequently, methods proposed for the PMSM may cause large error when applied to the MG. In [11], the field winding of the electrically excited synchronous machine (EESM) is used for signal detection, i.e., the stator is the transmitter and the rotor is the receiver. Initial rotor position estimation with this transmission direction is independent of the magnetic saliency and proven to be a suitable choice for the EESM [12]. Therefore, this transmission direction is also preferred for the initial rotor position estimation of the MG. However, methods proposed for the EESM cannot be applied to the MG directly, because the brushless structure prevents measurement of the field winding of the MG. To obtain the field winding information of the MG, a method is proposed in [13]. The field current of the MG is calculated with parameters and the rotor position of the ME. Unfortunately, the ME information needed in this method is usually not all available. In [14], when the BSSG is at standstill, the field current of the MG is estimated without knowing the rotor position of the ME. However, parameters of the ME are still needed and

978-1-5386-8330-9/19/$31.00 ©2019 IEEE

only simulation results are presented. As the rotor windings of the ME are connected with the rotating rectifier and cannot be measured, it is difficult to provide all the parameters needed in [14].

According to the measurability of parameters of the ME, a practical approach to estimate the field winding information of the MG is proposed in this paper. Then, signals are injected into the stator of the MG and response signals of the field winding are estimated and analyzed to detect the initial rotor position of the MG. An experimental platform is built to verify this method.

II. Estimation of the Field Winding Information of the MG at Standstill

The excitation system, shown in Fig. 2, of the BSSG consists of the ME, the field winding of the MG and the rotating rectifier. In Fig. 2, i_{esA}, i_{esB}, i_{esC} are the stator currents, i_{era}, i_{erb}, i_{erc} are the rotor currents, i_f is the field current of the MG, and θ_{er} is the rotor position. $\theta_{er} = \theta_{e0} + \omega_{er}t$, where θ_{e0} is the initial rotor position and ω_{er} is the rotor electrical angle velocity. According to the mathematical model of the ME, the rotor d- and q-axis currents are

$$i_{erd} = \frac{2}{3M_{esr}}\left[\int (u_{es\alpha} - R_{es}i_{es\alpha})dt - L_{es}i_{es\alpha}\right] \quad (1)$$

$$i_{erq} = \frac{2}{3M_{esr}}\left[\int (u_{es\beta} - R_{es}i_{es\beta})dt - L_{es}i_{es\beta}\right] \quad (2)$$

where R_{es} is the stator resistance, L_{es} is the stator inductance, and M_{esr} is the mutual inductance. i_{era}, i_{erb}, i_{erc} can be derived from the frame transformation

$$\begin{bmatrix} i_{era} \\ i_{erb} \\ i_{erc} \end{bmatrix} = \begin{bmatrix} \cos\theta_{er} & \sin\theta_{er} \\ -\sin\left(\theta_{er}+\frac{\pi}{6}\right) & \cos\left(\theta_{er}+\frac{\pi}{6}\right) \\ \sin\left(\theta_{er}-\frac{\pi}{6}\right) & -\cos\left(\theta_{er}-\frac{\pi}{6}\right) \end{bmatrix} \begin{bmatrix} i_{erd} \\ i_{erq} \end{bmatrix} \quad (3)$$

With the method in [13], the field current of the MG is

$$i_f = \frac{|i_{era}| + |i_{erb}| + |i_{erc}|}{2} \quad (4)$$

In equations (1)-(4), R_{es}, L_{es}, M_{esr}, and θ_{er} are essential to calculate i_f. At standstill, $\theta_{er} = \theta_{e0}$. With R_{es}, L_{es}, and M_{esr}, i_f can be estimated without knowing θ_{e0} [14]. Due to the extremely large inductance of the field winding of the MG and the rotating rectifier, the actual i_f is a dc current with a small amplitude ripple which is six times the frequency of the rotor currents of the ME [9], and this should also be the case with the estimated field current i_f^e (the superscript e denotes estimated variables). If θ_{e0}^e deviates from θ_{e0}, the ripple amplitude of i_f^e will increase. Therefore, i_f^e with the smallest ripple amplitude is the correct estimation result and the corresponding θ_{e0}^e can be used to estimate i_f at standstill. The same smallest ripple amplitude will be detected at six θ_{e0}^e with 60° interval, and the actual initial rotor position of the ME is one of them but cannot be identified. Fortunately, i_f can be estimated correctly with any one of the six positions [14].

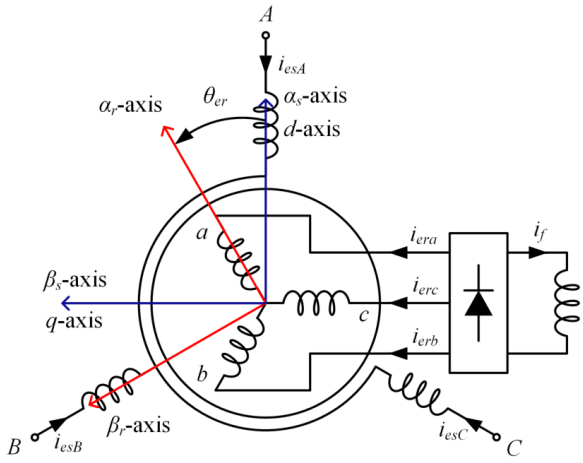

Fig. 2. Schematic of the excitation system of the BSSG.

Among the three parameters, R_{es} can be measured from the stator of the ME. To measure L_{es}, the BSSG can be driven to the same speed with the rotating magnetic field of the stator of the ME. Then, the currents of the rotor windings of the ME are zero and L_{es} can be measured with just currents and voltages of the stator windings of the ME. Since the rotor windings of the ME are connected with the rotating rectifier and difficult to measure, obtaining M_{esr} is a challenging job. From equations (1)-(4), it can be observed that M_{esr} is a scale factor multiplied in i_f^e. Thus, equations (1)-(4) are rewritten as equations (5)-(8). It should be mentioned that flux linkage variables in equations (5)-(8) are just symbols for calculation and may do not have clear physical meanings. With measured R_{es} and L_{es} of the ME, the field winding information, defined as ψ_f, of the MG can be estimated from equations (5)-(8) without knowing θ_{e0} when the BSSG is at standstill. i_f^e and ψ_f^e share same features and the only difference between them is a scale factor M_{esr}.

$$\psi_{erd} = i_{erd}M_{esr} = \frac{2}{3}\left[\int (u_{es\alpha} - R_{es}i_{es\alpha})dt - L_{es}i_{es\alpha}\right] \quad (5)$$

$$\psi_{erq} = i_{erq}M_{esr} = \frac{2}{3}\left[\int (u_{es\beta} - R_{es}i_{es\beta})dt - L_{es}i_{es\beta}\right] \quad (6)$$

$$\begin{bmatrix} \psi_{era} \\ \psi_{erb} \\ \psi_{erc} \end{bmatrix} = \begin{bmatrix} \cos\theta_{er} & \sin\theta_{er} \\ -\sin\left(\theta_{er}+\frac{\pi}{6}\right) & \cos\left(\theta_{er}+\frac{\pi}{6}\right) \\ \sin\left(\theta_{er}-\frac{\pi}{6}\right) & -\cos\left(\theta_{er}-\frac{\pi}{6}\right) \end{bmatrix} \begin{bmatrix} \psi_{erd} \\ \psi_{erq} \end{bmatrix} \quad (7)$$

$$\psi_f = \frac{|\psi_{era}| + |\psi_{erb}| + |\psi_{erc}|}{2} \quad (8)$$

III. Initial Rotor Position Estimation of the MG

The schematic of the MG is shown in Fig. 3, where i_A, i_B, i_C are the stator currents, u_A, u_B, u_C are the stator voltages, u_f is the field voltage, θ_0 is the initial rotor position, θ_0^e is the estimated initial rotor position, and $\Delta\theta_0$ is the difference between θ_0 and θ_0^e. When the BSSG is at standstill, the d-axis and the q-axis are decoupled, and only the d-axis is coupled with the field winding. When the sinusoidal voltage signal is injected into the d^e-axis, the current ripple with the same frequency will be induced in i_f and this information will also be included in ψ_f. When the resistive voltage drop is ignored, the induced ripple of ψ_f, defined as ψ_{fh}, can be approximately expressed as

$$\psi_{fh} = \frac{3M_{af}M_{esr}}{3M_{af}^2 - 2L_dL_{ff}} \frac{U_h}{2\pi f_h} \sin(2\pi f_h t)\cos(\Delta\theta_0) \quad (9)$$

where M_{af} is the mutual inductance, L_d and L_{ff} are the d-axis inductance and the field winding inductance, U_h and f_h are the amplitude and frequency of the injected sinusoidal voltage signal. From (9), the smaller the $\Delta\theta_0$, the higher the amplitude of ψ_{fh}. Therefore, the amplitude of ψ_{fh} can be used as the indicator for θ_0. When $\Delta\theta_0 = 0°$ or $180°$, the amplitudes of ψ_{fh} are the same. This $180°$ ambiguity can be eliminated by step signal injection. If a step voltage is injected, a sudden decrease of ψ_f will appear when $\Delta\theta_0 = 0°$, while a sudden increase of ψ_f will appear when $\Delta\theta_0 = 180°$. Therefore, θ_0 equals θ_0^e with the biggest amplitude of ψ_{fh} when the sinusoidal voltage is injected and a sudden decrease of ψ_f when the step voltage is injected.

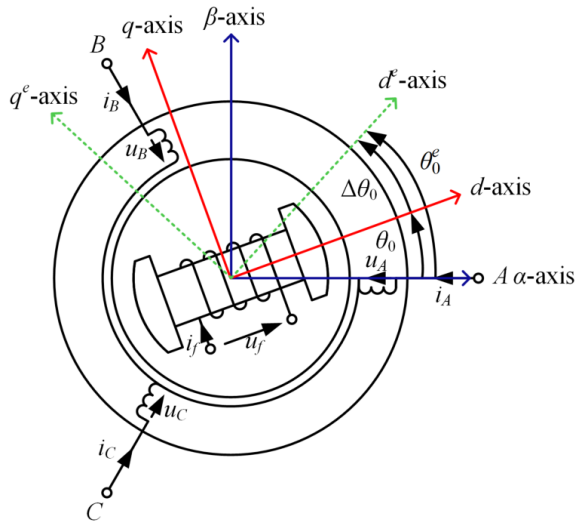

Fig. 3. Schematic of the MG of the BSSG.

IV. Experimental Results

The experimental setup is shown in Fig. 4. The BSSG consists of a three-phase wound-rotor induction machine (ME) and an electrically excited synchronous machine (MG). The rotor windings of the ME and the field winding of the MG are connected by a three-phase rectifier. Control algorithms are implemented on a RT-LAB system.

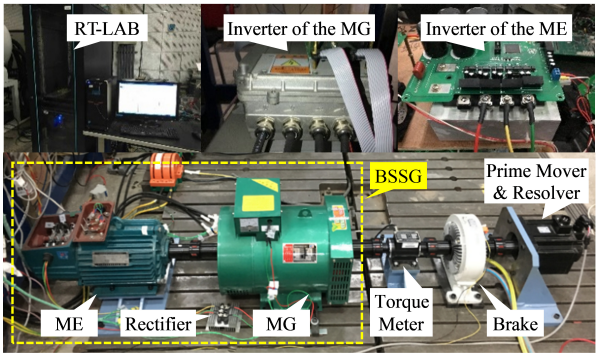

Fig. 4. Experimental setup.

R_{es} of the ME is about 4.72 Ω. To measure L_{es} of the ME, the BSSG is driven to the same speed with the rotating magnetic field of the stator of the ME. Then, with measured currents and voltages of the stator windings of the ME, L_{es} is estimated by the least square method. The estimation results are shown in Fig. 5 and L_{es} is about 0.29 H.

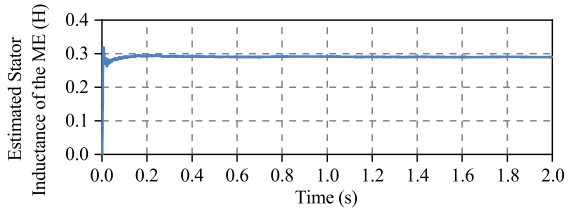

Fig. 5. Estimation results of the stator inductance of the ME.

To obtain θ_{e0}^e that is used to estimate the field winding information of the MG, a set of balanced 70 V/50 Hz three-phase voltages is applied to the stator windings of the ME. Then, θ_{e0}^e from 0° to 360° are used to estimate ψ_f with equations (5)-(8). Fast Fourier transform is performed to obtain the amplitude of the 300 Hz ripple of ψ_f^e at different θ_{e0}^e, and the results are shown in Fig. 6. It can be observed that six positions, 7.5°, 67.5°, 127.5°, 187.5°, 247.5° and 307.5°, are with the same smallest amplitude of the 300 Hz ripple. Fig. 7 shows that all the six positions have the same estimation result of ψ_f, so any one of them can be used to estimate ψ_f.

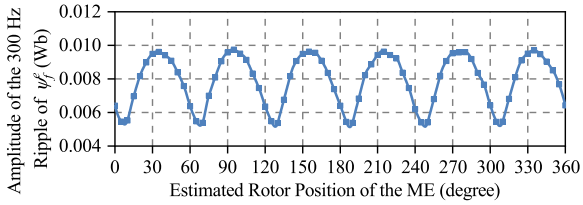

Fig. 6. Amplitude of the 300 Hz ripple of ψ_f^e at different θ_{e0}^e

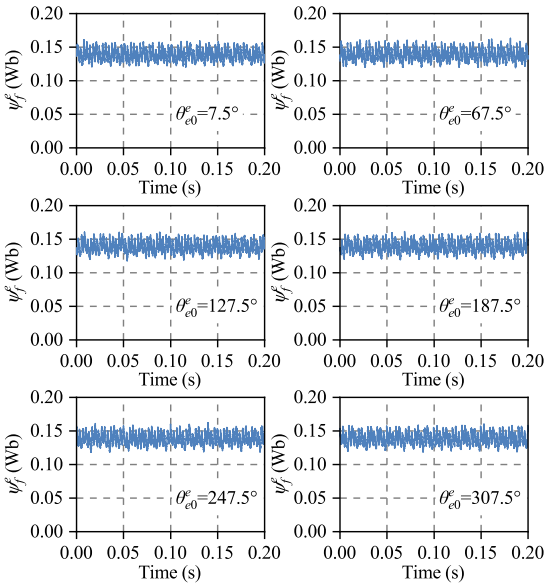

Fig. 7. ψ_f^e at the six θ_{e0}^e with the same smallest amplitude of the 300 Hz ripple.

A 40 V/500 Hz sinusoidal voltage is injected into the d^e-axis to estimate the initial rotor position of the MG. When θ_0^e are from 0° to 360°, the amplitude of ψ_{fh}, which is the 500 Hz ripple of ψ_f^e, is shown in Fig. 8 (a). The largest amplitude of ψ_{fh} occurs at two positions, 122° and 302°. Then, a 30V step voltage is injected at the two positions and the results are shown in Fig. 8 (b) and (c). The sudden decrease of ψ_f^e indicates 122° is correct. The actual initial rotor position of the MG is 120°, so the estimation error is about 2°. This estimation accuracy can meet the requirement of start control of the BSSG.

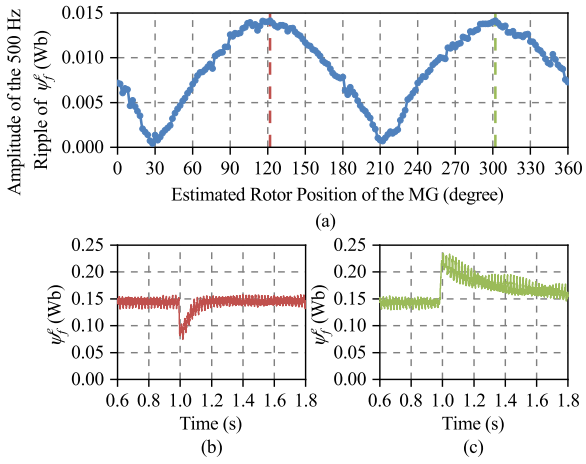

Fig. 8. (a): Amplitude of the 500 Hz ripple of ψ_f^e at different θ_0^e. (b): ψ_f^e at 122°. (c): ψ_f^e at 302°.

V. Conclusion

This paper has proposed a method to estimate the initial rotor position of the MG by signal injection. The stator and the rotor of the MG are the transmitter and the receiver respectively. The field winding information of the MG is estimated from the ME with measured parameters of the ME. The validity of the proposed method is verified by experimental results.

Acknowledgment

This work was supported by the National Natural Science Foundation of China (51677152).

References

[1] B. Sarlioglu and C. T. Morris, "More electric aircraft: Review, challenges, and opportunities for commercial transport aircraft," *IEEE Transactions on Transportation Electrification*, vol. 1, no. 1, pp. 54–64, June 2015.

[2] B. S. Bhangu and K. Rajashekara, "Electric starter generators: Their integration into gas turbine engines," *IEEE Industry Applications Magazine*, vol. 20, no. 2, pp. 14–22, March 2014.

[3] A. Griffo, R. Wrobel, P. H. Mellor, and J. M. Yon, "Design and characterization of a three-phase brushless exciter for aircraft starter/generator," *IEEE Transactions on Industry Applications*, vol. 49, no. 5, pp. 2106–2115, Sept 2013.

[4] J. Wei, Q. Zheng, M. Shi, B. Zhou, and J. Li, "The excitation control strategy of the three-stage synchronous machine in the start mode," in *2014 IEEE Applied Power Electronics Conference and Exposition - APEC 2014*, March 2014, pp. 2469–2474.

[5] N. Jiao, W. Liu, T. Meng, J. Peng, and S. Mao, "Design and control of a two-phase brushless exciter for aircraft wound-rotor synchronous starter/generator in the starting mode," *IEEE Transactions on Power Electronics*, vol. 31, no. 6, pp. 4452–4461, June 2016.

[6] Z. Zhang, W. Liu, D. Zhao, S. Mao, T. Meng, and N. Jiao, "Steady-state performance evaluations of three-phase brushless asynchronous excitation system for aircraft starter/generator," *IET Electric Power Applications*, vol. 10, no. 8, pp. 788–798, 2016.

[7] S. Mao, W. Liu, Z. Zhang, N. Jiao, and D. Zhao, "A torque ripple reduction method for the aircraft wound-rotor synchronous starter/generator in the starting mode," in *2018 IEEE Applied Power Electronics Conference and Exposition (APEC)*, March 2018, pp. 546–551.

[8] S. Feuersänger and M. Pacas, "Initial rotor position detection in synchronous machines using low frequency pulses," in *IECON 2014 - 40th Annual Conference of the IEEE Industrial Electronics Society*, Oct 2014, pp. 675–681.

[9] J. Wei, Y. Yang, B. Zhou, and J. Xue, "The integrated method of ac excitation and high-frequency signal injection for the sensorless starting control of brushless synchronous machines," in *IECON 2017 - 43rd Annual Conference of the IEEE Industrial Electronics Society*, Oct 2017, pp. 4188–4193.

[10] J. Peng, W. Liu, J. Meng, T. Meng, and G. Luo, "Initial orientation and sensorless starting strategy of wound-rotor synchronous starter/generator," in *2016 IEEE Applied Power Electronics Conference and Exposition (APEC)*, March 2016, pp. 2748–2753.

[11] A. Rambetius and B. Piepenbreier, "Carrier signal based sensorless control of wound field synchronous machines using the rotor winding as the receiver: Rotating vs. alternating carrier," in *Proceedings of PCIM Europe 2015; International Exhibition and Conference for Power Electronics, Intelligent Motion, Renewable Energy and Energy Management*, May 2015, pp. 1–8.

[12] ——, "Sensorless control of wound field synchronous machines for the whole speed range," in *Proceedings of PCIM Europe 2015; International Exhibition and Conference for Power Electronics, Intelligent Motion, Renewable Energy and Energy Management*, May 2015, pp. 1–8.

[13] P. C. Kjaer, T. Kjellqvist, and C. Delaloye, "Estimation of field current in vector-controlled synchronous machine variable-speed drives employing brushless asynchronous exciters," *IEEE Transactions on Industry Applications*, vol. 41, no. 3, pp. 834–840, May 2005.

[14] S. Mao, W. Liu, P. Ma, Z. Zhang, and Y. Hu, "Initial rotor position estimation method for aircraft wound-rotor synchronous starter/generators," *The Journal of Engineering*, vol. 2018, no. 13, pp. 541–545, 2018.